

Myoblasts inhibit prostate cancer growth by paracrine secretion of TNF alpha

Name of authors: **Meline N. L. Stölting¹, MD; Stefano Ferrari², PhD; Christoph Handschin³, PhD; Attila Becskei⁴, PhD; Maurizio Provenzano¹, MD. PhD; Tullio Sulser¹, Prof.; Daniel Eberli^{1*}, MD. PhD**

Name of institutions: ¹Laboratory for Urologic Tissue Engineering and Stem Cell Therapy, Division of Urology, University of Zurich, Frauenklinikstrasse 10, CH 8091 Zurich, Switzerland; ²Institute of Molecular Cancer Research, University of Zurich, Winterthurerstr 190, CH-8057 Zürich, Switzerland; ³Biozentrum, Focal Area Growth and Development, University of Basel, Klingelbergstrasse 50-70, CH-4056 Basel, Switzerland; ⁴Institute of Molecular Biology, University of Zurich, Winterthurerstr 190, CH-8057 Zürich, Switzerland

Published in J Urol. 2013 May;189(5):1952-9. PMID: 23123370. doi: 10.1016/j.juro.2012.10.071

Copyright © Elsevier; Journal of Urology

1 Title: **Myoblasts inhibit prostate cancer growth by paracrine secretion of TNF**
2 **alpha**

3 Name of authors: **Meline N. L. Stölting₁, MD; Stefano Ferrari₂, PhD; Christoph**
4 **Handschin₃, PhD; Attila Becskei₄, PhD; Maurizio Provenzano₁, MD. PhD; Tullio**
5 **Sulser₁, Prof.; Daniel Eberli_{1*}, MD. PhD**

6 Name of institutions: ₁Laboratory for Urologic Tissue Engineering and Stem Cell
7 Therapy, Division of Urology, University of Zurich, Frauenklinikstrasse 10, CH 8091
8 Zurich, Switzerland; ₂Institute of Molecular Cancer Research, University of Zurich,
9 Winterthurerstr 190, CH-8057 Zürich, Switzerland; ₃Biozentrum, Focal Area Growth
10 and Development, University of Basel, Klingelbergstrasse 50-70, CH-4056 Basel,
11 Switzerland; ₄Institute of Molecular Biology, University of Zurich, Winterthurerstr 190,
12 CH-8057 Zürich, Switzerland

13 *Corresponding Author: Daniel.Eberli@usz.ch, Phone: +41 44 255 9619, Fax: +41 44
14 255 9620

15 **Keywords:** Prostate cancer growth inhibition, myoblast transplantation for SUI,
16 metastasis hindrance.

17 **Word count (Abstract):** 299

18 **Word count (text):** 2680 (2381+ 299)

19 **Word count (Take Home Message):** 35

20

21 **ABSTRACT**

22 **Background:** Myoblasts are capable of forming muscle fibers after transplantation and
23 are therefore envisioned urinary incontinence treatment after radical prostatectomy.
24 However, the safety of this treatment and its interactions with putative remaining
25 neighboring cancer cells has not yet been investigated.

26 **Objective:** To determine the safety of myoblast transplantation for the treatment of
27 post-prostatectomy stress urinary incontinence by analyzing microenvironmental
28 interactions between myoblasts and prostate carcinoma cells *in vitro* and *in vivo*.

29 **Design, Setting and Participants:** Myoblasts isolated from *rectus abdominis* of
30 patients undergoing abdominal surgery were co-cultured with prostate cancer cells and
31 subcutaneously co-injected with tumor cells *in vivo*.

32 **Outcome Measurements and Statistical Analyses:** Cell proliferation, cycle arrest
33 and apoptosis of cancers in co-culture with myoblasts were performed. Tumor volume
34 and metastasis formation were evaluated in a mouse model. Tissue specific markers
35 were assessed by immunohistochemistry, FACS analyses, Western blot and RT-
36 qPCR. Outcome was statistically analysed by independent samples t-tests, one-way-
37 ANOVA and Pearson Correlation.

38 **Results and Limitations:** In this study we have demonstrated that myoblasts, in
39 proximity of tumor, provide paracrine TNF α to their microenvironment, decreasing
40 tumor growth of all prostate cancer cell lines examined. Co-culture experiments
41 showed induction of cell cycle arrest, tumor death by apoptosis and increased
42 differentiation of myoblasts. This effect was in large parts blocked by TNF α inhibition.
43 The same outcome was demonstrated in a mouse model, where co-injected human
44 myoblasts also inhibited tumor growth and metastasis formation of all prostate cancer
45 cell lines evaluated. This research is based on established models for cancer research.

46 However, the complex interactions between stromal and tumor cells were not
47 addressed.

48 **Conclusions:** Our results suggest that differentiating MPCs restrict tumor growth and
49 limit metastasis formation by paracrine TNF- α secretion and support the safety of
50 cellular therapy using myoblasts for muscle reconstruction, even in the proximity of
51 prostate cancer.

52

53 **TAKE HOME MESSAGE**

54 Differentiating MPCs restrict tumor growth and limit metastasis formation by
55 paracrine TNF- α secretion. This Indicates that the treatment of post prostatectomy
56 urinary incontinence with autologous myoblasts is safe, even in patients with
57 recurrent prostate cancer.

58

59 **INTRODUCTION**

60 Skeletal muscle comprises nearly 50% of the human body, is richly vascularized but
61 rarely the site of cancer metastases. The cellular and molecular mechanisms
62 underlying this phenomenon are not yet understood[1]. An intrinsic protective
63 mechanism avoiding ingrowth of metastatic cells and formation of new tumors seems
64 to be present. Simultaneously, skeletal muscles are the source of myoblasts[2],
65 which are capable of regenerating muscle fibers, and therefore are investigated for
66 the treatment of several muscular dysfunctions, including stress urinary incontinence
67 (SUI)[3], a frequent complication after radical prostatectomy[4]. Preclinical studies
68 have demonstrated that myoblasts, when implanted in the urinary sphincter,
69 efficiently recover continence [5]. The pelvic floor is also a frequent site of residual
70 prostate cancer cells[6], but until now no investigations targeted cell fate and possible
71 interactions between myoblasts and vicinal preexisting cancer.

72 Parallels have long been drawn between stem cells and cancer cells. In fact, both
73 cell types share common features such as capacity for self-renewal, differentiation
74 potential, relative quiescence, resistance to drug and toxins, resistance to apoptosis,
75 secretion of growth factors and stimulation of angiogenesis by production of vascular
76 endothelial growth factor (VEGF)[7]. These features could result in two possible
77 outcomes: Cell proliferation or cell death. For instance, the presence of VEGF, which
78 is secreted by many stem cells and progenitor cells including myoblasts[8], has the
79 potential to promote prostate cancer angiogenesis leading to enhanced tumor growth
80 and bone metastasis[9]. On the other hand, myoblasts are activated by
81 inflammation[2] and use inflammatory cytokines to perform and regulate their cross-
82 talk for activation and differentiation[10]. These same inflammatory cues, paracrine
83 secreted by myoblasts, could triggers cancer apoptosis.

84 A recent study successfully demonstrated inhibited growth of melanoma cells in the
85 presence of myoblasts, but failed to describe a possible intercellular mechanism that
86 explains this cell behavior [11]. Upon differentiation, myoblasts secrete tumor
87 necrosis factor alpha ($TNF\alpha$), which plays a key role in myoblast activation and
88 differentiation, thereby linking inflammation to muscle regeneration[12]. In tumor
89 cells, $TNF\alpha$ activates two parallel pathways, nuclear factor- κ B (NF- κ B) or c-Jun N-
90 terminal kinase (JNK). If NF- κ B is activated, $TNF\alpha$ acts as a growth promoter,
91 stimulating proliferation and metastasis. However, if JNK is turned on, a Caspase3-
92 dependent-apoptosis-pathway leads to cell death[13]. In this study, we demonstrate
93 that myoblast-secreted- $TNF\alpha$ is capable of influencing vicinal prostate carcinoma by
94 inducing cell cycle arrest and apoptosis *in vitro* and *in vivo*. Additionally, despite the
95 proximity to prostate cancer, myoblasts will rapidly differentiate into well-organized
96 myotubes. Cell-therapy with myoblasts might provide an ideal treatment of post-
97 prostatectomy urinary incontinence by improving sphincter function and inhibiting
98 potential recurrent prostate cancer in the pelvic floor.

99

100 **MATERIAL AND METHODS**

101

102 **Cell Isolation and Culture**

103 Upon ethical-approval and informed-consent, myoblasts were isolated from *rectus*
104 *abdominis* biopsies of male patients (60-80 y) undergoing abdominal surgery.

105 Biopsies were immediately processed according to established protocols[14] and
106 cells were expanded until passage 2 (P2) with a medium change every third day. Cell
107 characterization was performed by cellular growth rate, FACS analyses,
108 Immunocytochemistry, gene expression assay (RT-QPCR) and Western Blot. Muscle
109 tissue formation was assessed by injecting 5 million myoblasts with a collagen carrier
110 into the subcutaneous space of nude-mice. Tissues were retrieved after three and six
111 weeks for histological analysis.

112 The three prostate carcinoma cell lines (ATCC-LGC Standard) were chosen
113 according to their increasing clinical aggressiveness. They are retrieved from lymph
114 node (LNCaP)[15], bone (PC3) [16], and brain (DU145) metastasis[17]. An
115 aggressive vulvar leiomyosarcoma cell line (SK-LMS1) served as an additional
116 cancer control [18]. An indirect co-culture model (BD Falcon™) was applied, where
117 cells shared culture medium (DMEM enriched with 10% fetal bovine serum (FBS)
118 and 1% streptomycin/penicillin) thereby exchanging their cellular products without
119 direct cell-cell-contact. Cells were co-cultured for 10 day with medium change every
120 third day, and analyses performed at four time points (days 1, 4, 7 and 10). TNF α
121 was neutralized with a mouse monoclonal anti-TNF α antibody (Sigma, T-6817).

122

123 **Growth Rate and Fiber Formation Assay (FFA)**

124 Cells were trypsinized and hemocytometer cell counts were performed on triplicates,

125 averaged and growth curves were plotted by time (days). In all cases, triplicate
126 samples of log phase cells were plated at a density of 5×10^3 cells/cm². Cell viability
127 was confirmed by toluidine blue staining. The formation of myofibers was examined
128 on slide chambers and after 8 days in differentiating condition myofibers were fixed
129 (methanol, 7min), stained (1:20 Giemsa, 1h) and air dried. Images were taken with a
130 Leica-Imager-M1 Microscope. Five high-power-fields (HPF) were analyzed and data
131 expressed as fused cells in myofibers/HPF, number of fibers/HPF and cells per fiber.

132

133 FACS Analyses

134 Cells were immunolabeled by overnight incubation with anti-Pax7 (1:200, Sigma),
135 anti-MyoD (1:100, BD Pharmingen), anti-desmin (1:50, BDBiosciences), anti-MyHC
136 (1:4, DSHB) and anti-sarcomeric- α -actinin (1:1000, Sigma) and one hour with FITC-
137 Goat-Anti-mouse-IgG/IgM antibody (2ng/ μ l, BDBiosciences). A total of 50'000 events
138 were recorded by FACSCanto flow-cytometer (BDBiosciences) immediately after
139 labeling and data analyzed using FlowJo (7.1.3, Tree Star Inc.). All data are
140 expressed as percent positive cells as defined by flow-cytometry.

141

142 Western Blot

143 Cells were washed with PBS/protease inhibitor (Sigma) and lysed with lysis buffer
144 (50mM Tris-HCl, 150mM NaCl, 10% glycerol, 1% Triton X-100, 2mM EDTA, 40mM β -
145 glycerophosphate, 50mM sodium-fluoride, 10 μ g/ml leupeptin, 10 μ g/ml aprotinin, 1 μ M
146 pepstatinA, 1mM PMSF). Samples were centrifuged (10min, 13000rpm), and proteins
147 determined in the supernatant. Total protein was measured using DCTM Protein-
148 Assay (Bio-Rad), and 30 μ g of protein lysate was loaded on 12% Biorad gels.
149 Proteins were transferred onto PVDF-membranes (Millipore), blocked (1h, 5% non-

150 fat-dry-milk), and incubated (4°C, overnight) with anti-Desmin (1:100, BD
151 Biosciences), anti-MyH (1:6, DSHB), anti-TNF α (1:500, Sigma), anti-p21^{WAF1}
152 (1:1000, Calbiochem), Cleaved Caspase-3-Asp175 (1:1000, Cell- Signaling) and anti-
153 GAPDH (1:2000, Sigma). Membranes were washed (TBS-0.1% Tween-20, 30min),
154 incubated with HRP-conjugated secondary antibody (TBS-0.1% Tween-20, 5% non-
155 fat-dry-milk, 1 h) and developed by an ECL-technique (ECL-Kit, Amersham).

156

157 RT-qPCR

158 RNA extraction, cDNA preparation and RT-qPCR reactions were done using
159 Taqman® gene expression assay kits (Applied Biosystems), according to
160 manufacture's protocols. Data were normalized with 18S expression, quantitatively
161 analyzed by quantification cycles (C_q) and fold changes[19] and graphically
162 represented in amplification plots. MIQE guidelines were followed.

163

164 *In vivo* Experiments and Tumor Size Determination

165 Myoblasts and tumor cells were cultured as described above, mixed in a collagen
166 carrier (1mg/ml) and bilaterally injected into the dorsal subcutaneous space of 8
167 nude-mice (i.e. 16 samples) per group. Cell-cell interactions *in vivo* were examined
168 on day 21 and 42 after injection in nine groups: four with co-injected 5×10^6 myoblasts
169 and 2.5×10^6 cancer cells (LNCaP, PC3, DU145 and SK-LMS), four controls of the
170 respective tumors with 2.5×10^6 cancer cells alone, 1 myoblast control with 5×10^6
171 cells. The experiments were performed in time course triplicates and repeated with
172 four different patient myoblasts samples. Tumor volume and growth was measured
173 and volume was calculated according to the formula $\text{mm}^3 = a^2 \times b / 2$ [20]. Tumor/sample
174 size, myoblast differentiation, tumor aggressiveness and metastasis (lymph node,

175 lung and liver) were assessed after three and six weeks by histological staining of 10
176 μm thick frozen sections. Histomorphometric analysis was performed using the MBF
177 software "IMAGEJ for microscopy".

178

179 Histological Staining and Immunocytochemistry

180 Cells/tissues were fixed (4% PFA, 10min, RT), permeabilized (0,5% Triton, 7min),
181 blocked (5% BSA/0,1% Triton, RT, 30min) and immunolabelled with anti-Pax7
182 (1:200, Sigma), anti-MyoD (1:100, BD Pharmingen), anti-desmin (1:50, BDBiosciences),
183 anti-MyH (1:4, DSHB) and anti-sarcomeric actinin (1:1000, Sigma), and incubated 1
184 hour with anti-mouse-IgG-Cy3 (Sigma). Digital images were taken with a Leica
185 Imager M1 Microscope. Tissues were also stained with Hematoxylin and eosin (HE)
186 by incubating slides in hematoxylin (10min, water rinse 2min), dipping in 1% acid
187 alcohol and Eosin, and dehydrating with consecutive EtOH (70%, 96%, 100%) and
188 Xylol dips.

189

190 Statistics

191 Presented data are expressed as averages with corresponding standard deviation.
192 Analyses by independent samples t-tests, one way ANOVA or Pearson Correlation
193 were done with SPSS v20 (SPSS Inc, Chicago, IL). Graphics were drawn on the
194 GraphPad software Prism 5 for Windows. A $p < 0.05$ was considered significant.

195

196 **RESULTS**

197 **Myoblasts differentiate and cancer cells undergo cell cycle arrest and apoptosis in**
198 **co-culture *in vitro***

199 Human myoblasts were successfully isolated and characterized by FACS,
200 Immunocytochemistry (ICC) and Fiber Formation Assay (FFA). The cell population
201 expressed $76.5 \pm 2.3\%$ PAX-7, $60.6 \pm 6.3\%$ MyOD, and $81.6 \pm 2.5\%$ desmin. After
202 four days of co-culturing human myoblasts (Figure 1A, 1B) and prostate carcinoma
203 cell lines *in vitro* (Figure 1C, 1D), myoblasts displayed a decreasing growth rate
204 (Figure 1E), fused and developed muscle fibers and, therefore increasing (Figure 1F)
205 their differentiation ratio ($p < 0.001$). While only $4.2 \pm 1.0\%$ of the control myoblasts
206 formed muscle fibers, the differentiation ratio of myoblasts increased in parallel to the
207 respective prostate cancer line aggressiveness ($p = 0.011$), with rates of $11.5 \pm 5.5\%$ in
208 LNCaP, $14.5 \pm 6.9\%$ in PC3 and $25.3 \pm 2.3\%$ in DU145. Conversely, cancer cell lines
209 significantly decreased ($p < 0.001$) their growth rate (Figure 1G). The decrease in
210 cancer cell growth was due to cell cycle arrest and apoptosis (Figure 1H), as
211 demonstrated by Western Blot and RT-QPCR for Caspase 3 and p21^{WAF}.

212

213 **TNF α -dependent induction of cell cycle arrest and apoptosis in cancer cell lines co-**
214 **cultured with myoblasts.**

215 Myoblasts demonstrated a striking, up to 25 fold, increase of TNF α mRNA when
216 exposed to tumor (Figure 2A), which lead to significantly higher amounts of TNF α
217 ($p < 0.001$) into the conditioned-medium in the co-culture system (Figure 2B). The
218 myoblast-TNF α -secretion in co-culture increased gradually according to the
219 corresponding prostate carcinoma aggressiveness ($p < 0.001$), significantly correlating
220 (Pearson: 0.754, $p < 0.001$) with the myoblast differentiation ratio (Figure 2C). Yet, the

221 presence of prostate cancer induced higher autocrine-TNF α -secretion by myoblasts,
222 leading to robust muscle fiber formation. Furthermore, TNF α -antibody blocking
223 decreased the myoblast differentiation ratio and permitted cancer growth *de novo*
224 (Figure 2D) by reducing Caspase3 and p21^{WAF} mRNA and protein expression to
225 control-levels (Figure 2E). The myoblast-secreted-TNF α concentration negatively
226 correlated to cancer cell growth ($p < 0.001$, Pearson value -0.58) suggesting that
227 myoblast-paracrine-TNF α is sufficient to induce significant cancer growth inhibition. A
228 parallel assay demonstrated that cancer cell lines alone do not reach detectable
229 levels of TNF α RNA or protein expression.

230

231 Myoblast restrain tumor growth inducing cancer apoptosis and cell cycle arrest *in vivo*

232 Interactions between myoblasts and prostate cancer were further investigated *in vivo*
233 by co-injecting myoblasts and tumor cells subcutaneously in nude-mice (Figure 3A).
234 All co-injected samples reduced tumor growth ($p < 0.05$), while tumor injected alone
235 kept growing widely (Figure 3A, 3B). Although, no systemic metastasis could be
236 detected, prostate carcinoma infiltrated local lymph nodes (Figure 3C). Lymph node
237 micrometastasis were significantly reduced in co-injected groups (10,9%), when
238 compared to control (90,6%). These results demonstrate that myoblasts collaborate to
239 restrict prostate cancer to its primary site, thus significantly ($p < 0.001$) reducing
240 metastasis.

241 The extent to which myoblasts influenced cancer occurred gradually again following
242 cancer aggressiveness (Figure 4). Histomorphometric distance analyses
243 demonstrated that the tumor areas closer to the newly formed muscle underwent
244 apoptosis and cell cycle arrest more intensely (Pearson values -0.91 and -0.86
245 respectively) supporting the hypothesis that soluble factors are responsible for the

246 antitumor effects (Figure 5). Despite the evident changes in tumor behavior, muscle
247 tissue developed a well-organized and differentiated structure *in vivo*. We could not
248 detect any changes in muscle phenotype in the presence of tumor, which also
249 preserved a similar expression of Desmin and p21^{WAF}.

250

251 **DISCUSSION**

252 Cell-cell interactions play a crucial role in tissue formation, regeneration processes
253 and inflammatory reactions. Cellular signalling between neighboring cells is based on
254 two main mechanisms: Growth modulation by endogenous secretion of active
255 compounds and cell competition. These two mechanisms have been well
256 documented in fibroblasts, which are capable of secreting growth factors and other
257 peptides, thus delivering cues to neighboring cells. Fibroblasts isolated from breast
258 tumoral areas are permissive allowing breast cancer metastasis, whereas fibroblast
259 from normal breast tissue restrict tumor growth[21]. Cell competition has also been
260 proposed to regulate early cancer stages, when developing cancer cells overcome
261 genomic constraints[22]. It triggers apoptosis within and around tumors by promoting
262 rivalry between different anaplastic and normal cell lineages[23].

263 In this context, myoblasts also present key intercellular signaling products that allow
264 cross-talk required for myogenesis and new fiber formation upon muscle injury[24].

265 We demonstrated that myoblasts produce increased $\text{TNF}\alpha$ levels in the presence of
266 tumor cells, stimulating muscle differentiation and inducing cancer cell death.

267 Myoblasts secrete higher $\text{TNF}\alpha$ levels when differentiating and this paracrine-
268 secretion evokes microenvironmental changes, which control muscle regeneration by
269 activating Pax7 in quiescent myoblasts and thereby induce differentiation and muscle
270 formation[12]. We have demonstrated that myoblasts in co-culture with cancer cells
271 increase $\text{TNF}\alpha$ -secretion, inducing apoptosis *in vitro* and *in vivo*. $\text{TNF}\alpha$ bound to
272 TNFR-1 receptor triggers Caspase-3 activation leading to an apoptotic cascade and
273 cell death[25]. The dual effect of $\text{TNF}\alpha$ inducing differentiation in myoblasts and
274 apoptosis in tumors can be explained by two parallel pathways: activation of p38 α
275 and c-Jun N-terminal kinase (JNK). Once p38 α is activated, Pax7 initiates

276 myogenesis and myoblast differentiation[12] and, by activating the JNK pathway,
277 triggers cancer apoptosis through a Caspase-3-dependent pathway[13]. A further line
278 of action of TNF α in cancer inhibition affects tumor vascularity, probably due to
279 higher response to TNF α in tumoral vessels by receptor up-regulation (TNFR-1)[25].
280 These observations suggest that small amounts of TNF α delivered by differentiating
281 myoblasts can be enough to induce tumoral anti-vascular effects.

282 This research was based on established models for cancer research, however the
283 complex interactions between stromal and tumor cells were not addressed. We
284 demonstrated that myoblast-secreted-TNF α levels increase according to tumor
285 aggressiveness, in accordance with previous findings correlating prostate cancer
286 Gleason-score and inflammatory response to endogenous cytokines[26]. The
287 presence of inflammatory factors related to muscle regeneration plays a role in
288 myoblast-secreted-TNF α regulation[12]. This leads to the hypothesis that specific
289 inflammatory cues delivered by the prostate tumor stimulate neighboring myoblasts
290 to produce higher TNF α levels. A potential pathway is the increase of TACE
291 production due to stress and nutrient shortage, leading to increased release of
292 endogenous TNF α by muscle cells [27]. We anticipate that investigations targeting
293 cancer-mediated-stress factors on muscle cells will be the focus of future efforts
294 towards a better understanding of interactions between cancer and Adult Stem Cells,
295 such as myoblasts.

296 **CONCLUSIONS**

297 Myoblasts can be isolated from muscle biopsies of patients, rapidly grown in culture,
298 implanted into the site of injury and thereafter form functional muscle within weeks.

299 Our results indicate that differentiating myoblasts secret TNF α inducing apoptosis
300 and cell cycle arrest in Prostate cancer. These characteristics make myoblasts
301 promising cell source for muscle reconstruction, even in the proximity of cancer.

302 **ACKNOWLEDGEMENTS**

303 We gratefully acknowledge the technical assistance of Dr. Marten Schneider, Dr.
304 Irina Agarkova, Dr. Sousan Salemi and Fatma Kivrak on the improvement of our
305 FACS, IHC and WB methods. This work was supported by the Hartmann-Müller
306 Foundation, Forschungskredit, Swiss National Foundation and University of Zürich.

307

308 **REFERENCES**

309

310 [1] Plaza JA, Perez-Montiel D, Mayerson J, Morrison C, Suster S. Metastases to soft
311 tissue. *Cancer*. 2008;112:193-203.

312 [2] Gopinath SD, Rando TA. Stem Cell Review Series: Aging of the skeletal muscle
313 stem cell niche. *Aging Cell*. 2008;7:590-8.

314 [3] Carr L, Steele D, Steele S, et al. 1-year follow-up of autologous muscle-derived
315 stem cell injection pilot study to treat stress urinary incontinence. *International*
316 *Urogynecology Journal*. 2008;19:881-3.

317 [4] Klingler HC, Marberger M. Incontinence after radical prostatectomy: surgical
318 treatment options. *Current Opinion in Urology*. 2006;16:60-4.

319 [5] Eberli D, Aboushwareb T, Soker S, Yoo JJ, Atala A. Muscle Precursor Cells for
320 the Restoration of Irreversibly Damaged Sphincter Function. *Cell Transplantation*.
321 2012.

322 [6] Leventis AK, Shariat SF, Slawin KM. Local Recurrence after Radical
323 Prostatectomy: Correlation of US Features with Prostatic Fossa Biopsy Findings¹.
324 *Radiology*. 2001;219:432-9.

325 [7] Reya T, Morrison SJ, Clarke MF, Weissman IL. Stem cells, cancer, and cancer
326 stem cells. *Nature*. 2001;414:105-11.

327 [8] Mac Gabhann F, Ji JW, Popel AS. VEGF gradients, receptor activation, and
328 sprout guidance in resting and exercising skeletal muscle. *J Appl Physiol*.
329 2007;102:722-34.

330 [9] Carducci MA, Jimeno A. Targeting Bone Metastasis in Prostate Cancer with
331 Endothelin Receptor Antagonists. *Clin Cancer Res*. 2006;12:6296s-300.

332 [10] Dhawan J, Rando TA. Stem cells in postnatal myogenesis: molecular
333 mechanisms of satellite cell quiescence, activation and replenishment. *Trends in Cell*
334 *Biology*. 2005;15:666-73.

335 [11] Parlakian A, Gomaa I, Solly S, et al. Skeletal Muscle Phenotypically Converts
336 and Selectively Inhibits Metastatic Cells in Mice. *PLoS ONE*. 2010;5:e9299.

337 [12] Palacios D, Mozzetta C, Consalvi S, et al. TNF/p38[alpha]/Polycomb Signaling to
338 Pax7 Locus in Satellite Cells Links Inflammation to the Epigenetic Control of Muscle
339 Regeneration. *Cell stem cell*. 2010;7:455-69.

340 [13] Wang X, Lin Y. Tumor necrosis factor and cancer, buddies or foes[quest]. *Acta*
341 *Pharmacol Sin*. 2008;29:1275-88.

342 [14] Eberli D, Soker S, Atala A, Yoo JJ. Optimization of human skeletal muscle
343 precursor cell culture and myofiber formation in vitro. *Methods*. 2009;47:98-103.

344 [15] Horoszewicz JS, Leong SS, Kawinski E, et al. LNCaP Model of Human Prostatic
345 Carcinoma. *Cancer Research*. 1983;43:1809-18.

346 [16] Kaighn ME, Narayan KS, Ohnuki Y, Lechner JF, LW. J. Establishment and
347 characterization of a human prostatic carcinoma cell line (PC-3). *Investigative*
348 *Urology*. 1979;17:16-23.

349 [17] Stone KR, Mickey DD, Wunderli H, Mickey GH, DF. P. Isolation of a human
350 prostate carcinoma cell line (DU 145). *International journal of cancer*. 1978;21:274-
351 81.

352 [18] Fogh J FJ, Orfeo T. One hundred and twenty-seven cultured human tumor cell
353 lines producing tumors in nude mice. *Journal of the National Cancer Institute*.
354 1977;59:221-8.

- 355 [19] Schmittgen TD, Livak KJ. Analyzing real-time PCR data by the comparative C(T)
356 method. *Nat Protoc.* 2008;3:1101-8.
- 357 [20] Eva Corey, Janna E. Quinn, Kent R. Buhler, et al. LuCaP 35: A new model of
358 prostate cancer progression to androgen independence. *The Prostate.* 2003;55:239-
359 46.
- 360 [21] Dong-LeBourhis X, Berthois Y, Millot G, et al. Effect of stromal and epithelial
361 cells derived from normal and tumorous breast tissue on the proliferation of human
362 breast cancer cell lines in co-culture. *Int J Cancer.* 1997;71:42 - 8.
- 363 [22] Simpson P, Morata G. Differential mitotic rates and patterns of growth in
364 compartments in the *Drosophila* wing. *Developmental Biology.* 1981;85:299-308.
- 365 [23] Moreno E. Is cell competition relevant to cancer? *Nat Rev Cancer.* 2008;8:141-7.
- 366 [24] Chen S-E, Gerken E, Zhang Y, et al. Role of TNF- α signaling in
367 regeneration of cardiotoxin-injured muscle. *Am J Physiol Cell Physiol.*
368 2005;289:C1179-87.
- 369 [25] van Horssen R, ten Hagen TLM, Eggermont AMM. TNF- α in Cancer
370 Treatment: Molecular Insights, Antitumor Effects, and Clinical Utility. *Oncologist.*
371 2006;11:397-408.
- 372 [26] Nuñez C, Cansino JR, Bethencourt F, et al. TNF/IL-1/NIK/NF-kappaB
373 transduction pathway: a comparative study in normal and pathological human
374 prostate (benign hyperplasia and carcinoma). *Histopathology.* 2008;53:166-76.
- 375 [27] Zhan M, Jin B, Chen S-E, Reecy JM, Li Y-P. TACE release of TNF- α
376 mediates mechanotransduction-induced activation of p38 MAPK and myogenesis. *J*
377 *Cell Sci.* 2007;120:692-701.
- 378
- 379

380

381 **FIGURE LEGENDS**

382

383

384 **Figure 1 – Co-culture effects on myoblasts and cancer cells.** Cell growth rate,
385 differentiation ratio, morphology and gene expression were influenced by co-culture.
386 Myoblasts differentiated rapidly in the presence of tumor, significantly increasing
387 differentiation ratio (A, B, F) and, consequently, decreasing cell growth (E). Prostate
388 carcinoma and sarcoma cells significantly decreased in growth (C, D, G) and
389 underwent apoptosis and/or cell cycle arrest (C, D, H). Desmin staining in co-culture
390 (A) and control (B), Caspase 3 staining of DU145 cells in co-culture with myoblasts
391 (C) and control (D), cytoskeleton labelled in green (Phalloidin 488) and secondary
392 antibody in red (Cy3). Caspase 3 and p21 mRNA fold increase and protein
393 expression (H) significantly increased when compared to tumor control (dashed
394 line=1.0). Samples in co-culture with myoblast were represented as (+ Mb) and
395 control without myoblasts as (- Mb). mRNA fold increase was normalized with 18S
396 reference gene (*p<0.001, **p=0.005, ***p=0.011)

397

398 **Figure 2 – Myoblast secreted TNF α induce myoblast differentiation and inhibit**
399 **cancer cell line growth rate by inducing apoptosis and cell cycle arrest.** (A) RT-
400 QPCR assay demonstrates myoblast mRNA expression increase on the fourth day of
401 co-culture with different cancer cell lines. A significant difference could be found
402 between different prostate cancer cell lines, increasing according to tumor
403 aggressiveness. (B) Myoblasts TNF α secretion increases according to the cancer
404 aggressiveness in co-culture. CM: conditioned Medium. (C) Myoblast differentiation
405 ratio correlate (Pearson correlation: 0.754) to the amount of produced TNF α . (D)

406 Cell growth rate of cancer (LNCaP, PC3, DU145 and SK.LMS-1) was assessed by
407 cell counting at day 1, 4, 7 and 10 of co-culture. All cancer cell lines showed a
408 significant decrease in growth in the presence of myoblasts (bold lines), when
409 compared to control (fine line). Cancer growth rate was in great part recovered
410 (dashed lines) after $\text{TNF}\alpha$ neutralization. (E) Apoptosis and cell cycle arrest are
411 triggered in all cancer cells co-cultured with myoblasts. Again $\text{TNF}\alpha$ blocking in
412 conditioned medium reverse in great part these effects. Caspase 3 and p21 tumor
413 control mRNA fold increase is represented with a dashed line (=1.0). (* $p < 0.001$,
414 ** $p < 0.05$).

415

416 **Figure 3 – Tumor growth and lymph node metastasis was reduced *in vivo* in**
417 **samples co-injected with myoblasts.** (A) 21 days after subcutaneous cell injection,
418 tumor size was measured and a significant tumor size difference was found between
419 co-injected and control samples. On day 42, myoblast co-injected tumor mass
420 shrank, whereas control samples kept growing. (B) Final tumor size at day 42 was
421 significantly smaller in myoblast co-injected samples. (C) Axillar lymph node
422 metastasis assessment was performed by analysis of macro- and micrometastasis
423 with H&E, Desmin and cytokeratin staining, positive lymph nodes. Ratio of axillar
424 metastasis was also significantly reduced ($p < 0.001$) in all tested cancers, when co-
425 injected with myoblasts. Samples co-injected with myoblasts were represented as (+
426 Mb) and control without myoblasts as (- Mb). * $p < 0.05$, ** $p = 0.009$, *** $p = 0.002$

427

428 **Figure 04 – Histological aspect of subcutaneously injected tumor *in vivo*.** At day
429 42, HE staining demonstrates a tendency of newly formed muscle and cancer tissue
430 (first row) to growth in clusters, with differentiated muscle areas impairing growth of

431 neighbor tumor masses. In opposition, control cancers (second row) grow freely
432 forming bigger and complex tumor masses. Increasing Caspase3 and p21^{WAF}
433 expression was detected in all tumors in samples co-injected with myoblasts.
434 Samples co-injected with myoblasts were represented as (+ Mb) and controls are
435 cancer cell lines injected without myoblasts (-Mb). In the co-injected samples muscle
436 is represented with a "M" and cancer tissue areas with a "C". DAPI (blue), anti-mouse
437 IgG Cy3 (red), and the injected myoblasts were labelled *in vitro* with PKH 67 (green).
438 Muscle on

439

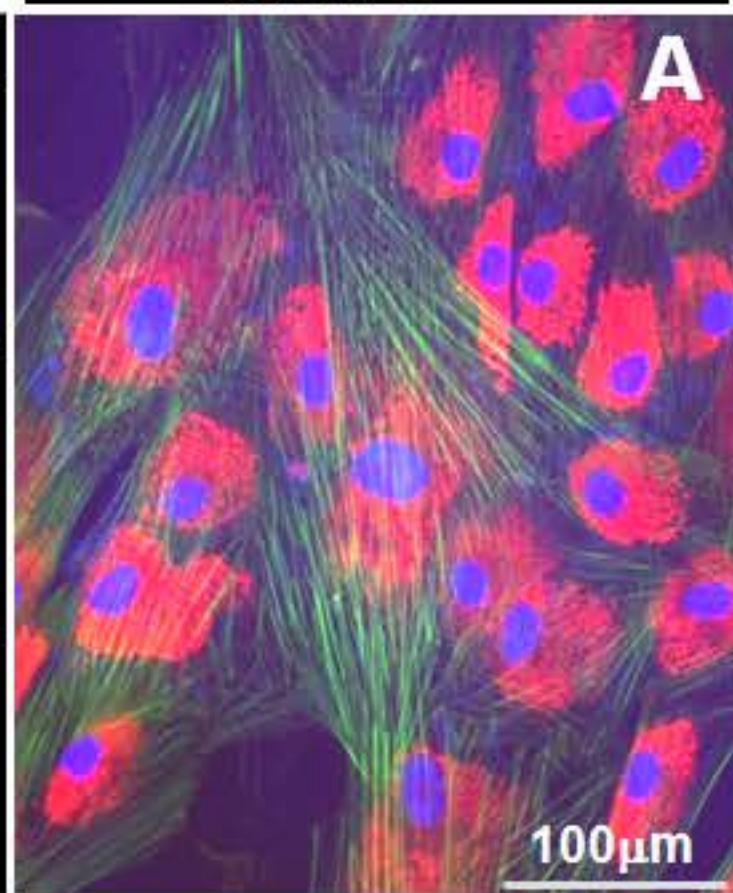
440 **Figure 05 – Histomorphometric analyses of co-injected tumor with myoblasts.**

441 Histomorphometric analysis demonstrates a significant increase on apoptosis (A) and
442 cell cycle arrest (B) in all tested tumors. (C) Three tumor areas were analyzed
443 according to distance of newly formed muscle. The total positive area, calculated by
444 fluorescence intensity, demonstrated a gradient of Caspase 3 and p21 expression in
445 all cancers tested. These directly correlated with the proximity to differentiating
446 muscle tissue. Samples co-injected with myoblast were represented as (+ Mb) and
447 control without myoblasts as (- Mb). *p<0.001, ** p< 0.05, ***p=0.001

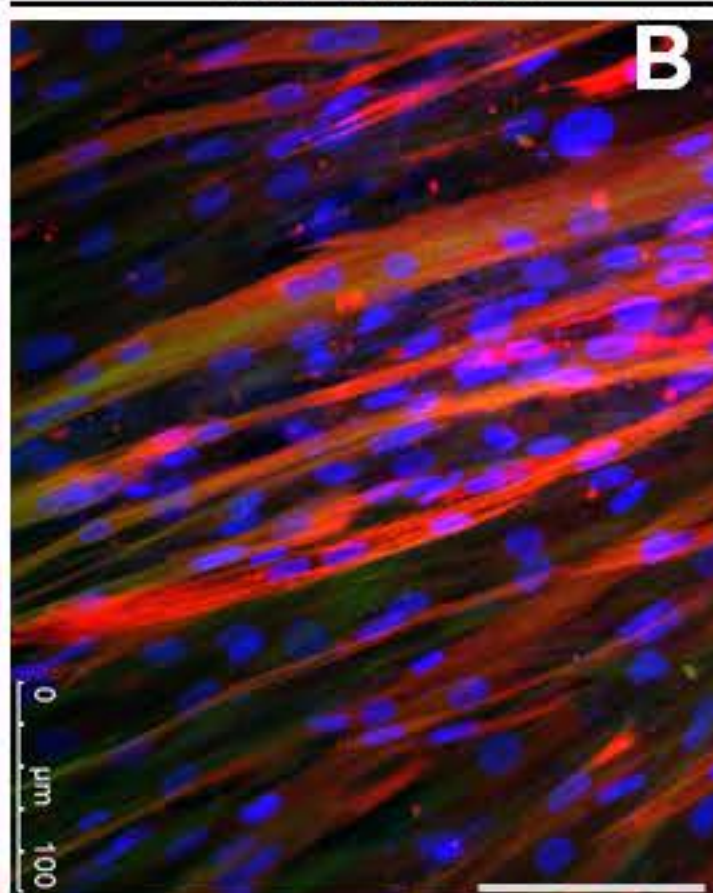
448

Myoblasts (Desmin)

control



Co-culture



DU145 (Caspase 3)

